J. Fluid Mech. (1978), *vol.* 85, *part* 2, *pp.* 325–347
Printed in Great Britain

The Wiener–Hermite expansion applied to decaying isotropic turbulence using a renormalized time-dependent base

By H. D. HOGGE† AND W. C. MEECHAM
School of Engineering and Applied Science, University of California, Los Angeles

(Received 22 June 1977)

The problem of decaying isotropic turbulence has been studied using a Wiener–Hermite expansion with a renormalized time-dependent base. The theory is largely deductive and uses no modelling approximations. It has been found that many properties of large Reynolds number turbulence can be calculated (at least for moderate time) using the moving-base expansion alone. Such properties found are the spectrum shape in the dissipation range, the Kolmogorov constant, and the energy cascade in the inertial subrange. Furthermore, by using a renormalization scheme, it is possible to extend the calculation to larger times and to initial conditions significantly different from the equilibrium form. If the initial spectrum is the Kolmogorov spectrum perturbed with a spike or dip in the inertial subrange, the process proceeds to eliminate the perturbation and relax to the preferred spectrum shape. The turbulence decays with the proper dissipation rate and several other properties are found to agree with measured data. The theory is also used to calculate the energy transfer and the flatness factor of turbulence.

1. Introduction

Based on the pioneering work of Wiener (1939, 1958) and Cameron & Martin (1947), a theory of turbulence, now called the Wiener–Hermite (WH) expansion, has been developed (see Imamura, Meecham & Siegel 1965; Meecham & Jeng 1958; Meecham & Clever 1971). The central idea is to expand the turbulent velocity field with respect to a complete set of stochastic functionals such that the first term in the expansion has Gaussian statistics and the higher-order terms represent deviations from Gaussianity. The expansion is in essence an expansion about Gaussianity designed to take advantage of the nearly Gaussian (in many ways) nature of turbulence. Two basic advantages of the WH theory should be emphasized: the results are necessarily realizable (all spectra are positive) and the theory is deductive, using no adjustable, or quasi-empirical, parameters.

The results obtained by applying the WH expansion to the initial-value problem of decaying Burgers' model turbulence (Jeng *et al.* 1966; Orszag & Bissonnette 1967; Crow & Canavan 1970) showed some defects. The theory breaks down at moderately large Reynolds numbers, or decay times, owing to the lack of rapid convergence required for truncation of the expansion to a computationally feasible number of terms (two

† Present address: Poseidon Research, 11777 San Vicente Boulevard, Los Angeles, California 90049.

terms is the realistic limit). Recent refinements in the theory making use of a convected set of base functionals (Clever & Meecham 1972), the moving base expansion, and later a renormalization scheme (Meecham 1972; Meecham, Iyer & Clever 1975) have demonstrated substantial improvement in the ability of the WH expansion to represent the decay of Burgers' model turbulence.

Except for a few limited computations (Meecham & Jeng 1968; Meecham & Clever 1971; Canavan 1970) the application of the WH expansion to the initial-value problem of the Navier–Stokes equations has not been demonstrated as thoroughly as for Burgers' model equation. Several investigators (Canavan 1970; Bodner 1969; Doi & Imamura 1969) have presented the theoretical background required to develop a convected base for the three-dimensional WH expansion but the application to the Navier–Stokes equations has yet to be demonstrated with a reasonable degree of success. The primary goal of this paper is to apply these more recent refinements of the WH expansion to the initial-value problem of decaying, isotropic, three-dimensional turbulence.

2. The vector Wiener–Hermite expansion

As indicated above, much of the work with the WH expansion has been done using the Burgers model equation. We shall not emphasize this work further, but proceed immediately to the three-dimensional turbulence problem. For the study of three-dimensional turbulence an expansion of the velocity vector as a random function of the position vector is required. The generalization of the scalar WH expansion to vector form has been presented previously (Imamura, Meecham & Siegel 1965). The basic element of the vector WH expansion is the three-dimensional ideal white noise process motivated by partitioning three-dimensional space into cubic cells of volume L^3, assigning to each cell an independent value chosen from a Gaussian distribution with zero mean and variance L^{-3}, and then letting L go to zero (see Meecham & Jeng 1968).

The three-dimensional ideal white noise process, denoted $H_i(\mathbf{x})$, has properties analogous to the scalar white noise process, $H(x)$. For example

$$\langle H_i(\mathbf{x})\rangle = 0, \tag{2.1}$$

and

$$\langle H_i(\mathbf{x}_1)\, H_j(\mathbf{x}_2)\rangle = \delta_{ij}\delta(\mathbf{x}_1-\mathbf{x}_2),$$

where the delta function with vector argument has been used to represent the product of delta functions of the three vector components. The bracket represents an ensemble average.

The basis functionals of the WH expansion are constructed as Hermite polynomial combinations of $H_i(\mathbf{x})$ as follows:

$$\left.\begin{aligned} H_i^{(1)}(\mathbf{x}) &= H_i(\mathbf{x}),\\ H_{ij}^{(2)}(\mathbf{x}_1,\mathbf{x}_2) &= H_i(\mathbf{x}_1)\, H_j(\mathbf{x}_2) - \delta_{ij}\delta(\mathbf{x}_1-\mathbf{x}_2),\\ H_{ijl}^{(3)}(\mathbf{x}_1,\mathbf{x}_2,\mathbf{x}_3) &= H_i(\mathbf{x}_1)\, H_j(\mathbf{x}_2)\, H_l(\mathbf{x}_3)\\ &\quad - H_i(\mathbf{x}_1)\,\delta_{jl}\delta(\mathbf{x}_2-\mathbf{x}_3) - H_j(\mathbf{x}_2)\,\delta_{il}\delta(\mathbf{x}_1-\mathbf{x}_3) - H_l(\mathbf{x}_3)\,\delta_{ij}\delta(\mathbf{x}_1-\mathbf{x}_2), \text{ etc.} \end{aligned}\right\} \tag{2.2}$$

The vector WH functionals have properties analogous to those of the scalar WH functionals; for example (suppressing subscripts), $\langle H^{(n)}(\cdot)\rangle = 0$ for all $n > 0$ and $\langle H^{(m)}(\cdot)\, H^{(n)}(\cdot)\rangle = 0$ if $m \neq n$.

The vector WH expansion for a homogeneous velocity field with zero mean is†

$$\begin{aligned} u_i(\mathbf{x}) = &\int K_{ij}^{(1)}(\mathbf{x}-\mathbf{x}')\, H_j^{(1)}(\mathbf{x}')\, d\mathbf{x}' \\ &+\iint K_{ijl}^{(2)}(\mathbf{x}-\mathbf{x}', \mathbf{x}-\mathbf{x}'')\, H_{jl}^{(2)}(\mathbf{x}', \mathbf{x}'')\, d\mathbf{x}', d\mathbf{x}'' \\ &+ \ldots . \end{aligned} \tag{2.3}$$

The kernels are non-random tensor functions of vector arguments.

For the study of homogeneous turbulence, it is more convenient to work in wavenumber space. Let the following quantities be defined as generalized Fourier transforms as follows (we shall truncate the series after the second term):

$$\left.\begin{aligned} u_i(\mathbf{x}) &= \left(\frac{1}{2\pi}\right)^3 \int \exp(-i\mathbf{k}.\mathbf{x})\, u_i(\mathbf{k})\, d\mathbf{k}, \\ K_{ij}^{(1)}(\mathbf{x}) &= \left(\frac{1}{2\pi}\right)^3 \int \exp(-i\mathbf{k}.\mathbf{x})\, K_{ij}^{(1)}(\mathbf{k})\, d\mathbf{k}, \\ H_j^{(1)}(\mathbf{x}) &= \left(\frac{1}{2\pi}\right)^3 \int \exp(-i\mathbf{k}.\mathbf{x})\, H_j^{(1)}(\mathbf{k})\, d\mathbf{k}, \\ K_{ijl}^{(2)}(\mathbf{x}_1, \mathbf{x}_2) &= \left(\frac{1}{2\pi}\right)^6 \iint \exp[-i(\mathbf{k}_1.\mathbf{x}_1 + \mathbf{k}_2.\mathbf{x}_2)]\, K_{ijl}^{(2)}(\mathbf{k}_1, \mathbf{k}_2)\, d\mathbf{k}_1\, d\mathbf{k}_2, \\ H_{jl}^{(2)}(\mathbf{x}_1, \mathbf{x}_2) &= \left(\frac{1}{2\pi}\right)^6 \iint \exp[-i(\mathbf{k}_1.\mathbf{x}_1 + \mathbf{k}_2.\mathbf{x}_2)]\, H_{jl}^{(2)}(\mathbf{k}_1, \mathbf{k}_2)\, d\mathbf{k}_1\, d\mathbf{k}_2. \end{aligned}\right\} \tag{2.4}$$

Taking the Fourier transforms of (2.1) and using the definitions above we get

$$\langle H_i(\mathbf{k})\rangle = 0, \tag{2.5a}$$

and

$$\langle H_i(\mathbf{k}_1)\, H_j(\mathbf{k}_2)\rangle = (2\pi)^3 \delta_{ij}\, \delta(\mathbf{k}_1 + \mathbf{k}_2). \tag{2.5b}$$

Likewise, for the Fourier transforms of (2.2) we get

$$H_i^{(1)}(\mathbf{k}) = H_i(\mathbf{k}), \tag{2.6a}$$

and

$$H_{ij}^{(2)}(\mathbf{k}_1, \mathbf{k}_2) = H_i(\mathbf{k}_1)\, H_j(\mathbf{k}_2) - (2\pi)^3 \delta_{ij}\, \delta(\mathbf{k}_1 + \mathbf{k}_2). \tag{2.6b}$$

Furthermore, the orthogonality properties of the WH functionals in wavenumber space are the same as in physical space.

If each of the definitions given in (2.4) are substituted into (2.3) and the resulting equation is Fourier transformed, the following WH expansion in wavenumber space is obtained:

$$\begin{aligned} u_i(\mathbf{k}) = &K_{ij}^{(1)}(\mathbf{k})\, H_j^{(1)}(\mathbf{k}) \\ &+ \left(\frac{1}{2\pi}\right)^3 \int K_{ijl}^{(2)}(\mathbf{k}-\mathbf{k}', \mathbf{k}')\, H_{jl}^{(2)}(\mathbf{k}-\mathbf{k}', \mathbf{k}')\, d\mathbf{k}' \\ &+ \ldots . \end{aligned} \tag{2.7}$$

3. Application to the Navier–Stokes equations

The first two terms of the WH expansion of the generalized Fourier transform of velocity for homogeneous turbulence with zero mean velocity are given by (2.7) where $K^{(1)}$ and $K^{(2)}$ are the first and second WH kernels and are deterministic (i.e. not

† Throughout this paper, the integral symbol without limits is used to symbolize integration over all three-dimensional space.

random) functions of wave vector and time. $H^{(1)}$ is the (Fourier transformed) three-dimensional white noise process and $H^{(2)}$ is the first non-Gaussian WH functional given by (2.6*b*). Equation (2.7) *et seq.* are implicitly time dependent (though time is not usually shown as an explicit argument).

The incompressible Navier–Stokes equations in wavenumber space with the pressure term eliminated by using the continuity equation are

$$k_i u_i(\mathbf{k}) = 0, \tag{3.1a}$$

and

$$((\partial/\partial t) + k^2\nu)\, u_i(\mathbf{k}) = \tfrac{1}{2}i(1/2\pi)^3 P_{ijl}(\mathbf{k}) \int u_j(\mathbf{k}-\mathbf{q})\, u_l(\mathbf{q})\, d\mathbf{q}, \tag{3.1b}$$

where the incompressibility tensors are defined as

$$P_{ijl}(\mathbf{k}) = k_j P_{il}(\mathbf{k}) + k_l P_{ij}(\mathbf{k}), \tag{3.2a}$$

and

$$P_{ij}(\mathbf{k}) = \delta_{ij} - k_i k_j / k^2. \tag{3.2b}$$

By substituting (2.7) into (3.1) we obtain an equation for the WH kernels. By using the statistical orthogonality of the WH functionals, this equation can be separated into two independent equations for the two WH kernels. The prodecure is as follows: first multiply by $H_r^{(1)}(\mathbf{p})$, average, use (2.5) and (2.6) to eliminate terms, and integrate over $\mathbf{p}$ to obtain the first equation; then multiply by $H_{rs}^{(2)}(-\mathbf{k}_1, -\mathbf{k}_2)$ and repeat the process (integrating over $\mathbf{k}$ and $\mathbf{q}$) to obtain the second equation. The two resulting equations for the two WH kernels are

$$\begin{aligned}
&\left(\frac{\partial}{\partial t} + k^2\nu\right) K_{ir}^{(1)}(\mathbf{k}) - 2i\left(\frac{1}{2\pi}\right)^3 P_{ijl}(\mathbf{k}) \int K_{jm}^{(1)}(\mathbf{k}')\, K_{lrm}^{(2)}(\mathbf{k}, -\mathbf{k}')\, d\mathbf{k}' \\
&\quad = \int K_{ij}^{(1)}(\mathbf{k}) \langle H_r^{(1)}(\mathbf{p})\, \dot{H}_j^{(1)}(\mathbf{k})\rangle\, d\mathbf{p} \\
&\qquad + \left(\frac{1}{2\pi}\right)^3 \iint K_{ijl}^{(2)}(\mathbf{k}-\mathbf{k}', \mathbf{k}') \langle H_r^{(1)}(p)\, \dot{H}_{jl}^{(2)}(\mathbf{k}-\mathbf{k}', \mathbf{k}')\rangle\, d\mathbf{k}'\, d\mathbf{p},
\end{aligned} \tag{3.3}$$

and

$$\begin{aligned}
&\left(\frac{\partial}{\partial t} + |\mathbf{k}_1 + \mathbf{k}_2|^2 \nu\right) K_{irs}^{(2)}(\mathbf{k}_1, \mathbf{k}_2) \\
&\quad - \tfrac{1}{2}i(\mathbf{k}_1 + \mathbf{k}_2)_l P_{ij}(\mathbf{k}_1 + \mathbf{k}_2) [K_{js}^{(1)}(\mathbf{k}_2)\, K_{lr}^{(1)}(\mathbf{k}_1) + K_{jr}^{(1)}(\mathbf{k}_1)\, K_{ls}^{(1)}(\mathbf{k}_2)] \\
&\quad + 2i\left(\frac{1}{2\pi}\right)^3 (\mathbf{k}_1 + \mathbf{k}_2)_l P_{ij}(\mathbf{k}_1 + \mathbf{k}_2) \int [K_{lrm}^{(2)}(\mathbf{k}_1, -\mathbf{k}')\, K_{jsm}^{(2)}(\mathbf{k}_2, \mathbf{k}') \\
&\quad + K_{lsm}^{(2)}(\mathbf{k}_2, -\mathbf{k}')\, K_{jrm}^{(2)}(\mathbf{k}_1, \mathbf{k}')]\, d\mathbf{k}' \\
&\quad = \tfrac{1}{2}(2\pi)^3 \int K_{ij}^{(1)}(\mathbf{k}) \langle H_{rs}^{(2)}(-\mathbf{k}_1, -\mathbf{k}_2)\, \dot{H}_j^{(1)}(\mathbf{k})\rangle\, d\mathbf{k} \\
&\qquad + \tfrac{1}{2} \iint K_{ijl}^{(2)}(\mathbf{k}-\mathbf{k}', \mathbf{k}') \langle H_{rs}^{(2)}(-\mathbf{k}_1, -\mathbf{k}_2)\, \dot{H}_{jl}^{(2)}(\mathbf{k}-\mathbf{k}', \mathbf{k}')\rangle\, d\mathbf{k}\, d\mathbf{k}'.
\end{aligned} \tag{3.4}$$

In (3.3) and (3.4) there are terms involving time derivatives of the WH functionals which cannot be evaluated from the basic properties of the expansion. These terms have been written on the right-hand sides of (3.3) and (3.4). In the original formulation of the WH expansion (Imamura *et al.* 1965; Meecham & Jeng 1968), the WH functionals were assumed to be independent of time. For this formulation, the fixed base formulation, the terms on the right-hand sides of (3.3) and (3.4) vanish and these

equations form a closed system for the first two WH kernels. Given initial values for the first two kernels, these equations can be integrated forward in time and hence provide a solution to the problem of decaying homogeneous turbulence. The validity of the solution is, of course, contingent on rapid enough convergence of the WH expansion to justify truncation to two terms. (A three-term solution would seem out of the question since the third WH kernel is a fourth-order tensor function of three vector arguments.) Based on the observed fact that turbulence is nearly Gaussian in many respects, it is not unreasonable to expect the required rapid convergence of the WH expansion.

It should be noted at this point that knowledge of the WH kernels is indeed a solution of the problem since any moment of the velocity field (and hence any measure of the turbulence) can be calculated in terms of the kernels. (In fact, the kernels can be used to calculate the members of the ensemble themselves.) For example, the energy spectrum – kinetic energy per unit mass per wavenumber – is given by (for isotropic turbulence)

$$\begin{aligned} E(k) &= 2\pi k^2 \Phi_{ii}(\mathbf{k}), \\ &= 2\pi k^2 \left(\frac{1}{2\pi}\right)^6 \int \langle u_i(\mathbf{k})\, u_i(\mathbf{k}')\rangle \, d\mathbf{k}', \\ &= \left(\frac{k}{2\pi}\right)^2 |K_{ij}^{(1)}|^2 + \frac{2k^2}{(2\pi)^5} \int |K_{ijl}^{(2)}(\mathbf{k}-\mathbf{k}', \mathbf{k}')|^2 \, d\mathbf{k}', \\ &= E_1(k) + E_2(k). \end{aligned} \tag{3.5}$$

That part of the energy spectrum resulting from $K^{(1)}$, denoted $E_1(k)$, has in the past been referred to as 'Gaussian energy'. That part resulting from $K^{(2)}$, denoted $E_2(k)$, has in the past been referred to as 'non-Gaussian energy'. As will be discussed in §4, however, these phrases are no longer considered appropriate. We shall refer to $E_1(k)$ as first-term energy and to $E_2(k)$ as second-term energy.

An additional characteristic of turbulence which will be found of interest is the energy transfer, $T(k)$, found by manipulating the Navier–Stokes equations into energy form to get

$$\begin{aligned} T(k) &= \left(\frac{\partial}{\partial t} + 2k^2\nu\right) E(k) \\ &= \frac{ik^2}{(2\pi)^8} P_{ijl}(\mathbf{k}) \iint \langle u_i(\mathbf{k}'')\, u_j(\mathbf{k}-\mathbf{k}')\, u_l(\mathbf{k}')\rangle \, d\mathbf{k}'\, d\mathbf{k} \\ &= 4\pi i k^2 P_{ijl}(\mathbf{k}) \int [2K_{im}^{(1)}(\mathbf{k})\, K_{jn}^{(1)}(\mathbf{k}')\, K_{lmn}^{(2)}(\mathbf{k}, \mathbf{k}') \\ &\quad + K_{imn}^{(2)}(-\mathbf{k}', \mathbf{k}'-\mathbf{k})\, K_{jm}^{(1)}(\mathbf{k}')\, K_{ln}^{(1)}(\mathbf{k}-\mathbf{k}')] \, d\mathbf{k}' + O(K^{(2)})^3. \end{aligned} \tag{3.6}$$

Since proper behaviour of the WH expansion seems to imply $K^{(2)} \ll K^{(1)}$, it will be assumed that the term cubic in $K^{(2)}$ is negligible. The energy transfer is perhaps the most important characteristic of turbulence because it contains the lowest-order information related to the nonlinear, non-Gaussian modal interaction process. For this reason we shall consider $T(k)$ to be the characteristic third-order moment.

4. The principal difficulty with the Wiener–Hermite expansion

As mentioned in the introduction, the WH expansion (and in particular, the fixed base formulation) has been unable to model the decay of homogeneous Burgers model turbulence for significant Reynolds numbers. The principal difficulty has been a loss of convergence due to the transfer of energy from the first kernel into the higher kernels. This cascading of energy through the expansion is necessary for a finite correlation time and is evidence of the fact that the WH expansion is not unique. Even if a random process is Gaussian, it is not required to have zero higher-order terms, even though the higher-order terms are themselves (slightly) non-Gaussian. A Gaussian process can be represented either by the first term alone, or by the first term along with a non-zero contribution from the higher terms. The situation is analogous to that of choosing co-ordinate axes to represent a vector: if a co-ordinate axis is chosen along the vector, the vector has but one component; on the other hand, if not, it may have many components. The difficulty involved in modelling the dynamics of a given process has been that of the tendency for energy to cascade from the first term into the higher terms even though the process remains nearly Gaussian. From this discussion it should be obvious that it is not proper to refer to E_1 as 'Gaussian' energy and to refer to E_2 as 'non-Gaussian' energy. The loss of Gaussian energy to the higher terms was the major difficulty with the fixed base analysis of decaying Burgers model turbulence. The problem was more pronounced for moderate, or larger, Reynolds numbers or decay times.

To overcome this difficulty (with the fixed base WH expansion) two basic changes are needed: first, we must use the 'moving base' analysis mentioned in the introduction wherein the WH functionals are allowed to change with time in such a way that they 'convect with the flow' thereby retaining as much as possible of the Gaussian energy in the first term; then we must use the concept of renormalization as applied (Meecham 1972; Meecham *et al.* 1975) to the Burgers model problem. This latter concept (renormalization) is the following: suppose, for simplicity, we begin the problem with all of the Gaussian energy in the first term and integrate forward using the moving base expansion (to prevent, as much as possible, the transfer of Gaussian energy out of the first term). When, after some time, a significant amount of Gaussian energy has cascaded from the first term into the higher terms in spite of our efforts, we stop the integration process and redistribute the energy content of the expansion in such a way that we keep the total energy the same, minimize the high-order contribution to the energy, and minimize the unwanted changes in other measurable quantities, such as the third-order moments, of the process. By following this procedure, a significant improvement in the ability of the WH expansion to model the decay of homogeneous Burgers model turbulence has been achieved (Meecham 1972; Meecham *et al.* 1975). The application of this renormalization procedure to the problem of three-dimensional decaying isotropic turbulence is the principal new achievement of this research.

5. The moving base expansion

In the most primitive form of the WH expansion, the fixed base expansion, the base functionals were held independent of time and all of the time variation of the expansion was captured in the kernels. The inability of the expansion in this form to model the

decay process of turbulence is well documentated (Orszag & Bissonnette 1967; Crow & Canavan 1970). Wiener himself recognized the difficulty of this fixed base approach and suggested that the base functionals be allowed to convect with the process being modelled. Doi & Imamura (1969) formulated the moving base approach by defining the time derivative of the three-dimensional ideal white noise process as follows:

$$\dot{H}_i(\mathbf{k}) = \int L_{ijl}(\mathbf{k}-\mathbf{k}', \mathbf{k}')\, H^{(2)}_{jl}(\mathbf{k}-\mathbf{k}', \mathbf{k}')\, d\mathbf{k}'. \tag{5.1}$$

They derived the symmetry condition on L (which is otherwise arbitrary) that guarantees that the base is undergoing a measure-preserving transformation in time so that all expectation values derived from the physical process are independent of L. In terms of L the right-hand side of (3.3) is

$$-4\int L^{(s)}_{mrn}(\mathbf{k}, -\mathbf{k}')\, K^{(2)}_{imn}(\mathbf{k}-\mathbf{k}', \mathbf{k}')\, d\mathbf{k}',$$

and the right-hand side of (3.4) is

$$(2\pi)^3 L^{(s)}_{mrs}(\mathbf{k}_1, \mathbf{k}_2)\, K^{(1)}_{im}(\mathbf{k}_1+\mathbf{k}_2),$$

where $$L^{(s)}_{ijl}(\mathbf{k}_1, \mathbf{k}_2) = \tfrac{1}{2}[L_{ijl}(\mathbf{k}_1, \mathbf{k}_2) + L_{ilj}(\mathbf{k}_2, \mathbf{k}_1)].$$

By requiring that (3.3) and (3.4) admit the Gaussian equipartition solution of the inviscid Navier–Stokes equation, Bodner (1969) and Doi & Imamura (1969) derived the following for L:

$$L_{ijl}(\mathbf{k}_1, \mathbf{k}_2) = i\left(\frac{1}{2\pi}\right)^3 (\mathbf{k}_1+\mathbf{k}_2)_n\, P_{mi}(\mathbf{k}_1+\mathbf{k}_2)\, P_{ml}(\mathbf{k}_2)\, K^{(1)}_{nj}(\mathbf{k}_1). \tag{5.2}$$

In terms of this moving base the differential equations for the WH kernels are

$$\left(\frac{\partial}{\partial t} + k^2\nu\right) K^{(1)}_{ir}(\mathbf{k}) - 2i\left(\frac{1}{2\pi}\right)^3 P_{ijl}(\mathbf{k}) \int K^{(1)}_{jm}(\mathbf{k}')\, K^{(2)}_{lrm}(\mathbf{k}, -\mathbf{k}')\, d\mathbf{k}'$$
$$= -2i\left(\frac{1}{2\pi}\right)^3 k_m P_{nr}(\mathbf{k}) \int P_{jn}(\mathbf{k}-\mathbf{k}')\, K^{(1)}_{ml}(\mathbf{k}')\, K^{(2)}_{ijl}(\mathbf{k}-\mathbf{k}', \mathbf{k}')\, d\mathbf{k}', \tag{5.3}$$

and

$$\left(\frac{\partial}{\partial t} + |\mathbf{k}_1+\mathbf{k}_2|^2\nu\right) K^{(2)}_{irs}(\mathbf{k}_1, \mathbf{k}_2)$$
$$-\tfrac{1}{2}i(\mathbf{k}_1+\mathbf{k}_2)_l P_{ij}(\mathbf{k}_1+\mathbf{k}_2)\,[K^{(1)}_{js}(\mathbf{k}_2)\, K^{(1)}_{lr}(\mathbf{k}_1) + K^{(1)}_{jr}(\mathbf{k}_1)\, K^{(1)}_{ls}(\mathbf{k}_2)]$$
$$+2i\left(\frac{1}{2\pi}\right)^3 (\mathbf{k}_1+\mathbf{k}_2)_l P_{ij}(\mathbf{k}_1+\mathbf{k}_2) \int [K^{(2)}_{lrm}(\mathbf{k}_1, -\mathbf{k}')\, K^{(2)}_{jsm}(\mathbf{k}_2, \mathbf{k}')$$
$$+K^{(2)}_{lsm}(\mathbf{k}_2, -\mathbf{k}')\, K^{(2)}_{jrm}(\mathbf{k}_1, \mathbf{k}')]\, d\mathbf{k}'$$
$$= -\tfrac{1}{2}i(\mathbf{k}_1+\mathbf{k}_2)_l K^{(1)}_{ij}(\mathbf{k}_1+\mathbf{k}_2)\,[P_{jm}(\mathbf{k}_2)\, K^{(1)}_{ln}(\mathbf{k}_1) + P_{jn}(\mathbf{k}_1)\, K^{(1)}_{lm}(\mathbf{k}_2)]. \tag{5.4}$$

6. Renormalization

Any moment of the random process can be calculated directly from the WH kernels. Examples shown in the preceding sections were the energy spectrum, $E(k)$, given by (3.5) and the energy transfer, $T(k)$, given by (3.6). The inverse problem is not so obvious. For example, suppose the random process were characterized to third order by specification of the second- and third-order moments $E(k)$ and $T(k)$. Can (3.5) and (3.6) be inverted to calculate the first and second WH kernels corresponding to the specified

$E(k)$ and $T(k)$? These equations are, after all, two equations for the two unknowns $K^{(1)}$ and $K^{(2)}$. Besides the obvious mathematical complexity apparent in (3.5) and (3.6), there is the basic question of uniqueness of the expansion itself. As stated before, a given random process does not have a unique WH expansion. As an obvious result, (3.5) and (3.6) cannot be inverted to give unique $K^{(1)}$ and $K^{(2)}$ for specified $E(k)$ and $T(k)$. In some sense, there must be a family of solutions to this problem. If we attempt to invert this set of equations, we shall ultimately have to choose one member of the solution family. And how shall we choose a member? It seems obvious that we should choose the one which optimizes the convergence of the WH expansion (i.e. maximize E_1 and minimize E_2). This optimization concept is the central idea of the renormalization technique.

The concept of renormalization as outlined in the previous sections is as follows: we begin the problem with all of the Gaussian energy in the first term and integrate forward using the moving base expansion (to prevent as much as possible the transfer of Gaussian energy out of the first term). When, after some time, a significant amount of Gaussian energy has cascaded from the first term into the higher terms we stop the integration process and redistribute the energy content of the expansion in such a way that we optimize the convergence without changing the moments of the random process. To second order in the WH series, the only moments of the random process are a second-order moment, e.g. $E(k)$, and a third-order moment, e.g. $T(k)$. Hence the renormalization is nothing more than solving the inverse problem of (3.5) and (3.6) for specified $E(k)$ and $T(k)$. The effectiveness of this procedure as a means of solving the initial-value problem of decaying isotropic turbulence will be demonstrated in the following sections.

An exact inverse of (3.5) and (3.6) by pure analysis does not seem possible. As a reasonable alternative we have developed the following approximate technique: as a first approximation, assume $\tilde{K}^{(2)} \approx 0$ and solve (3.5) for $\tilde{K}^{(1)}$; then assume a form for $\tilde{K}^{(2)}$ with arbitrary constants to be determined by a least-square optimization procedure which simultaneously minimizes $\tilde{E}_2$ (holding E fixed) and optimizes the fit to (3.6) (with $\tilde{K}^{(1)}$ used for $K^{(1)}$); finally the newly calculated $\tilde{K}^{(2)}$ is substituted into (3.5) and a refined $\tilde{K}^{(1)}$ is calculated. The tilde over a symbol is used throughout to represent quantities after renormalization. The set of kernels found in this way optimizes the convergence of the WH expansion, matches perfectly the second-order moment, $E(k)$, and minimizes the error in matching the third-order moment, $T(k)$.

To proceed as outlined above, let us first of all assume that the turbulence is isotropic so we can write the first kernel using a scalar generator $\tilde{U}(k)$ as follows:

$$\tilde{K}^{(1)}_{ij}(\mathbf{k}) = \tilde{U}(k)\, P_{ij}(\mathbf{k}). \tag{6.1}$$

The second kernel is more complicated – a third-order tensor function of two vector arguments. Meecham & Jeng (1968) have shown that $K^{(2)}$ can be written as a combination of four scalar generating functions. If we (in keeping with the truncation assumption) suppose that $\tilde{K}^{(2)}$ is small and hence that the terms in (5.4) quadratic in $\tilde{K}^{(2)}$ can be neglected, then $\tilde{K}^{(2)}$ can be written in terms of one scalar function as follows (assuming we begin with $\tilde{K}^{(2)} = 0$ at time t_0):

$$\tilde{K}^{(2)}_{ijl}(\mathbf{k}_1, \mathbf{k}_2) = i(\mathbf{k}_1 + \mathbf{k}_2)_m\, P_{in}(\mathbf{k}_1 + \mathbf{k}_2)\, [P_{mj}(\mathbf{k}_1)\, P_{nl}(\mathbf{k}_2)\, \tilde{F}(\mathbf{k}_1, \mathbf{k}_2) + P_{nj}(\mathbf{k}_1)\, P_{ml}(\mathbf{k}_2)\, \tilde{F}(\mathbf{k}_2, \mathbf{k}_1)]. \tag{6.2}$$

The differential equation for $\tilde{F}$ is

$$\left(\frac{\partial}{\partial t}+|\mathbf{k}_1+\mathbf{k}_2|^2\nu\right)\tilde{F}(\mathbf{k}_1,\mathbf{k}_2)=\tfrac{1}{2}\tilde{U}(k_1)[\tilde{U}(k_2)-\tilde{U}(|\mathbf{k}_1+\mathbf{k}_2|)]. \tag{6.3}$$

Integrating (6.3), we have

$$\tilde{F}(\mathbf{k}_1,\mathbf{k}_2)=\frac{1}{2}\int_{t_0}^{t}\exp[|\mathbf{k}_1+\mathbf{k}_2|^2\nu(t'-t)]\,\tilde{U}(k_1,t')[\tilde{U}(k_2,t')-\tilde{U}(|\mathbf{k}_1+\mathbf{k}_2|,t')]\,dt'.$$

Using the mean value theorem, we have

$$\tilde{F}(\mathbf{k}_1,\mathbf{k}_2)=\tfrac{1}{2}\bar{U}(k_1)[\bar{U}(k_2)-\bar{U}(|\mathbf{k}_1+\mathbf{k}_2|)]\frac{1-\exp[|\mathbf{k}_1+\mathbf{k}_2|^2\nu(t_0-t)]}{|\mathbf{k}_1+\mathbf{k}_2|^2\nu},$$

where $\bar{U}(k)$ is a characteristic 'mean value' of $\tilde{U}(k)$ for the time interval $[t_0,t]$. For large Reynolds numbers the multiplicative factor above can be replaced by a constant; hence, the function $\tilde{F}$ can be approximated by

$$\tilde{F}(\mathbf{k}_1,\mathbf{k}_2)=\tfrac{1}{2}W(k_1)[W(k_2)-W(|\mathbf{k}_1+\mathbf{k}_2|)], \tag{6.4}$$

where $W(k)$ is a scalar function to be determined. Representing $W(k)$ as an expansion with respect to some set of base functions $\{f_n(k)\}$, we have

$$W(k)=\sum_{n=1}^{N}a_n f_n(k). \tag{6.5}$$

Substituting (6.5) into (6.4) we have

$$\tilde{F}(\mathbf{k}_1,\mathbf{k}_2)=\frac{1}{2}\sum_{m=1}^{N}\sum_{n=1}^{N}a_m a_n[f_m(k_1)f_n(k_2)-f_m(k_1)f_n(|\mathbf{k}_1+\mathbf{k}_2|)].$$

Defining $A_{mn}=a_m a_n$ we have

$$\tilde{F}(\mathbf{k}_1,\mathbf{k}_2)=\sum_{mn=1}^{N^2}A_{mn}g_{mn}(\mathbf{k}_1,\mathbf{k}_2), \tag{6.6}$$

where

$$g_{mn}(\mathbf{k}_1,\mathbf{k}_2)=\tfrac{1}{2}f_m(k_1)[f_n(k_2)-f_n(|\mathbf{k}_1+\mathbf{k}_2|)]. \tag{6.7}$$

Since $\tilde{F}$ is linear in A and $\tilde{E}_2$ is quadratic in $\tilde{F}$, we can write $\tilde{E}_2$ as the following quadratic form:

$$\tilde{E}_2=\int_0^\infty\tilde{E}_2(k)\,dk=\sum_{ij=1}^{N^2}\sum_{mn=1}^{N^2}A_{ij}A_{mn}e_{ij,mn}, \tag{6.8}$$

where $e_{ij,mn}$ are simply integrals of g_{ij} and g_{mn}. The energy transfer, on the other hand, is linear in $\tilde{F}$ and hence is linear in A. Thus $\tilde{T}$ can be written in the form

$$\tilde{T}(k)=\sum_{ij=1}^{N^2}A_{ij}\tilde{t}_{ij}(k), \tag{6.9}$$

where $\tilde{t}_{ij}$ are integrals of $\tilde{U}$ and g_{ij}. We have for the error due to the approximation

$$\epsilon(k)=T(k)-\tilde{T}(k). \tag{6.10}$$

The total squared error in energy transfer is

$$\begin{aligned}\epsilon^2&=\int_0^\infty\epsilon(k)^2\,dk\\&=\int_0^\infty T(k)^2\,dk-2\sum_{mn=1}^{N^2}A_{mn}\int_0^\infty T(k)\tilde{t}_{mn}(k)\,dk\\&\quad+\sum_{ij=1}^{N^2}\sum_{mn=1}^{N^2}A_{ij}A_{mn}\int_0^\infty\tilde{t}_{ij}(k)\tilde{t}_{mn}(k)\,dk.\end{aligned} \tag{6.11}$$

If we want to minimize $\tilde{E}_2$ and ϵ^2 simultaneously we must introduce a weighting parameter Λ and solve for A_{ij} such that

$$(1-\Lambda)\frac{\partial \tilde{E}_2}{\partial A_{ij}} + \Lambda \frac{\partial \epsilon^2}{\partial A_{ij}} = 0. \tag{6.12}$$

This Λ gives the weight assigned to the two simultaneous minimizations. Substituting (6.8) and (6.11) into (6.12), we have

$$\sum_{mn=1}^{N^2} \left[\int_0^\infty \bar{l}_{ij}(k)\bar{l}_{mn}(k)\,dk + \left(\frac{1-\Lambda}{\Lambda}\right)\left(\frac{e_{ij,mn}+e_{mn,ij}}{2}\right)\right] A_{mn} = \int_0^\infty T(k)\bar{l}_{ij}(k)\,dk. \tag{6.13}$$

Equation (6.13) is a linear system to be solved for A_{ij} thereby producing $\tilde{F}$. Then (3.5) is used to recalculate $\tilde{U}(k)$ thus completing the inverse solution to (3.5) and (3.6) for the specified $E(k)$ and $T(k)$.

7. Computational results using the moving base without renormalization

We have solved the initial-value problem consisting of (5.3) and (5.4) (ignoring the term quadratic in $K^{(2)}$) and the following initial conditions: $K^{(2)}$ was set to zero and $K^{(1)}$ was chosen so that the energy spectrum was (the Kolmogorov form)

$$E(k) = a\frac{u_0^2}{k_0}\left(\frac{k}{k_0}\right)^4\left[b^2+\left(\frac{k}{k_0}\right)^2\right]^{-\frac{17}{6}} \tag{7.1}$$

This form of the energy spectrum was chosen to give k^4 behaviour for small k and $k^{-\frac{5}{3}}$ behaviour for large k. The constants a and b were chosen to be 1·09 and 0·645 by requiring $E(k)$ to peak at k_0 and to integrate to $(\frac{3}{2})u_0^2$. It should be noted that we have chosen non-equilibrium initial conditions by choosing zero $K^{(2)}$ and hence zero third (and higher odd) order moments. We expect the differential equations to generate an equilibrium state by the appropriate evolution of $K^{(2)}$. We have chosen an initial energy spectrum which has the presumed $k^{-\frac{5}{3}}$ equilibrium shape in the inertial subrange but does not have the viscous cut-off.

We have solved the initial-value problem described above (at least for moderate time) for three values of the initial Reynolds number: $Re = u_0/k_0\nu$ = 100, 1000, and 10000. The resulting one-dimensional energy spectra are shown in figure 1. The one-dimensional energy spectrum was chosen because this quantity is most easily compared with measured data. The energy spectra are non-dimensionalized in 'universal equilibrium' form and are compared with the same quantity obtained from two experiments (Grant, Stewart & Moilliet 1961; Kistler & Vrebalovich 1966). The solid lines are the calculated spectra and the symbols are the measured data points. The calculation has been quite successful in capturing the following features of the universal equilibrium spectrum: (1) the wavenumber of the viscous cut-off, (2) the spectrum shape in the far dissipation range, and (3) the amplitude constant (Kolmogorov constant) appearing in the energy spectrum. The arbitrary initial value of the Kolmogorov constant was (see the dashed line in figure 1) several times the correct value – which is then later calculated. The fact that the energy spectrum normalized in this way is properly scaled also indicates that the energy dissipation has been properly calculated. An earlier, very preliminary, effort was made to apply the moving-base procedure to the Navier–Stokes equation (Meecham & Clever 1971), but it failed because of computational difficulties, since resolved.

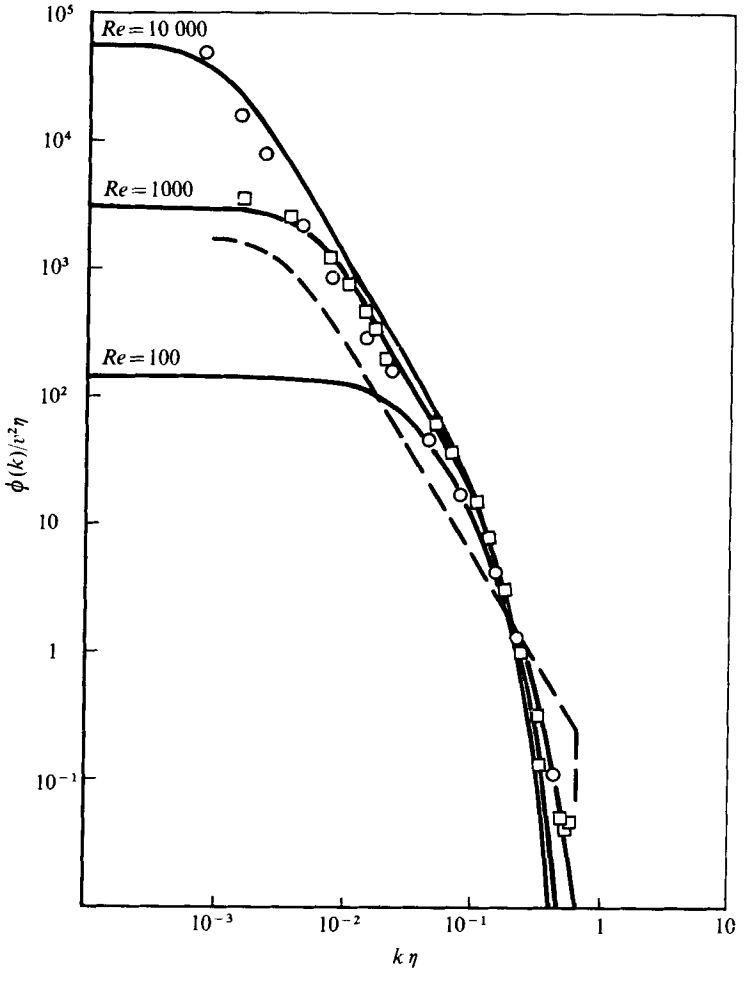

FIGURE 1. One-dimensional spectra normalized in universal equilibrium form. Solid lines are calculated spectra for Reynolds numbers indicated. Dashed line is initial spectrum for $Re = 1000$. Symbols are measured data: □, from Kistler & Vrebalovich (1966); ○, from Grant, Stewart & Moilliet (1961).

These results are not yet a complete solution to the problem of decaying isotropic turbulence. As discussed previously, the principal difficulty with the WH expansion is the transfer of energy out of the first term and the consequent breakdown of the expansion, even though the process remains approximately Gaussian. In fact, the rate of breakdown increases with Reynolds number. The results shown in figure 1 are for dimensionless times $u_0 k_0 t = 0{\cdot}5$, $0{\cdot}5$, and $0{\cdot}15$ for $Re = 100$, 1000, and 10000. These times seem to be the limit of the simple moving base analysis for $Re = 1000$ and 10000; without renormalization, the calculation breaks down at later times.

It is noted that these results are obtained using an arbitrary initial constant times the (correct) $k^{-\frac{5}{2}}$ spectrum. The moving base expansion cannot recover from an initial spectrum which is too far from its equilibrium form because significant contributions from (neglected) high-order terms are required during adjustment to equilibrium. It is significant, however, that in such a short time the analysis has been able to generate

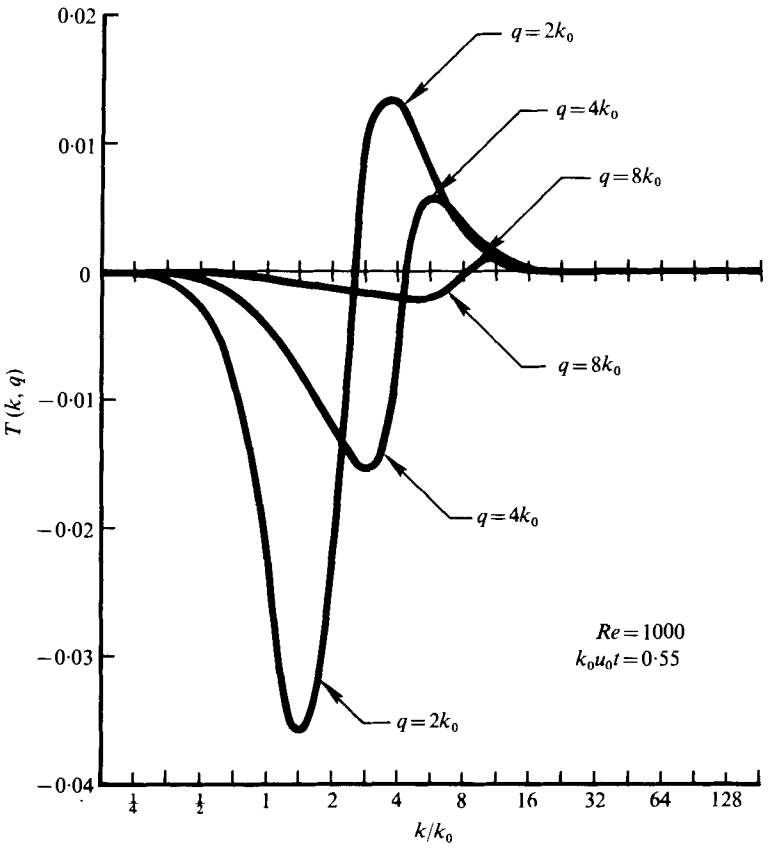

FIGURE 2. Energy transfer in the inertial subrange. $T(k, q)$ is the energy transferred from wavenumber q into wavenumber k.

correctly two important aspects of the energy spectrum: the viscous cut-off and the Kolmogorov constant.

Perhaps as significant as the results presented above for the energy spectrum, is the third-order moment (initially zero) generated by the analysis. Consider the energy transfer as an integral:

$$T(k) = \int_0^\infty T(k, q)\, dq, \tag{7.2}$$

where

$$T(k, q) = 8\pi^2 i k^2 P_{ijl}(\mathbf{k}) \int_0^\pi \{2K^{(1)}_{im}(\mathbf{k})\, K^{(1)}_{jn}(\mathbf{q})\, K^{(2)}_{lmn}(\mathbf{k}, \mathbf{q}) + K^{(2)}_{imn}(-\mathbf{q}, \mathbf{q}-\mathbf{k}) \times K^{(1)}_{jm}(\mathbf{q})\, K^{(1)}_{ln}(\mathbf{k}-\mathbf{q})\} \sin\theta\, d\theta.$$

The angle θ is the angle between the vectors $\mathbf{k}$ and $\mathbf{q}$.

The double wavenumber energy transfer $T(k, q)$ can be interpreted as the energy transferred from wavenumber q into wavenumber k. The result of calculating $T(k, q)$ from the same initial-value problem considered above for $Re = 1000$ and for time $u_0 k_0 t = 0{\cdot}55$ is shown in figure 2 for three values of q in the inertial subrange ($q = 2k_0$, $4k_0$, and $8k_0$). The result is a dramatic demonstration of the energy cascade in the inertial subrange. It is seen that the wavenumber q receives energy from the wave-

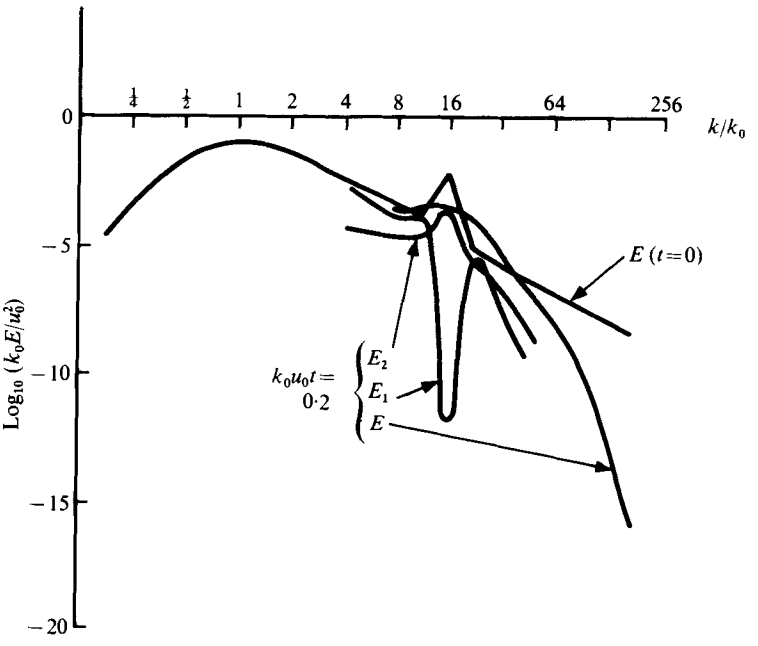

FIGURE 3. Evolution of a spectrum that initially had a bump in the inertial subrange.

numbers within approximately one octave below, and transfers energy to the wavenumbers within approximately one octave above.

As a final example using the moving base analysis alone, the following reveals the nature of the transfer of Gaussian energy out of the first term. Consider the same initial-value problem as before except for an artificial spike, doubling the equilibrium spectrum, in the inertial subrange. Figure 3 shows both the initial spectrum and the spectrum at time $u_0k_0t = 0{\cdot}2$. In addition to the generation of the viscous cut-off, the analysis has proceeded to smooth out and reduce the spike. The spectrum is attempting to evolve into the equilibrium form. An interesting phenomenon is the detailed nature of the evolution. At the wavenumber of the spike, the first-term energy E_1 has taken a large dip and the second-term energy E_2 is essentially the total energy. The conjecture is that the relative magnitudes of E_1 and E_2 are not necessarily indicative of the relative Gaussian and non-Gaussian content of the spectrum. In fact, all calculations of this type thus far indicate the same trend: the reduction of E_1 is greatest for the wavenumber range where the energy spectrum departs most from the equilibrium form. It seems that, whenever it is necessary to transfer energy from one wavenumber to another in order to achieve the equilibrium form, the expansion prefers to make that transfer from the first term into the higher terms instead of between wavenumbers in the first term.

8. Results for renormalization

We have applied the renormalization principle to the initial-value problem considered in the preceding section. The case of an initial Reynolds number $Re = 1000$ and a later time $u_0k_0t = 0{\cdot}25$ was selected. For this case $E_1k_0/u_0^2 = 1{\cdot}03$, and $E_2k_0/u_0^2 = 0{\cdot}26$

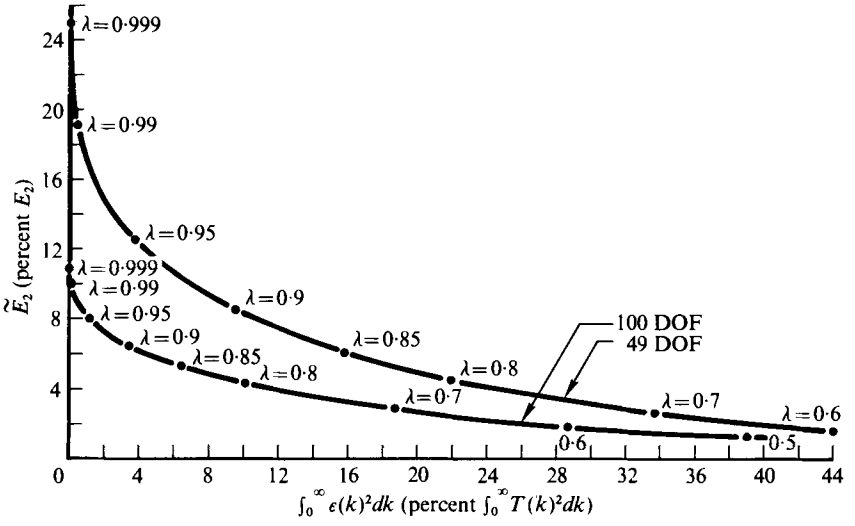

FIGURE 4. Renormalization performance map.

before renormalization. The wavenumber axis was partitioned into a set of 10 approximately octave band histograms to produce the set of base functions $f_n(k)$ used in (6.5). In terms of this set of base functions, the assumed form of $K^{(2)}$ has 100 unknown constants which must be found by solving (6.13). This will be referred to as a 100 degree-of-freedom (DOF) renormalization.

Since the renormalization is an attempt to minimize $\tilde{E}_2$ and the error produced in $T(k)$ simultaneously, we shall represent the effectiveness of the renormalization by a 'performance map' consisting of a plot of $\tilde{E}_2$ *vs.* energy transfer error. Such a performance map for the case considered here is shown in figure 4. We have plotted $\tilde{E}_2$ (after renormalization) as a percentage of E_2 before renormalization *vs.* the mean-squared energy transfer error as a percentage of the integral of the square of $T(k)$. The lower curve is the performance map of the 100 DOF renormalization with Λ [see (6.13)] as a parameter. The upper curve is the corresponding performance map of a 49 DOF (i.e. 7 histograms) renormalization of the same case.

As can be seen from figure 4, reasonably small energy transfer can be achieved only for Λ slightly less than unity (because, of course, of the relative size of the functions involved). For example, the error is insignificant for $\Lambda = 0{\cdot}999$ and yet the resulting $\tilde{E}_2$ is only 11 % of the E_2 before renormalization. The results are not as good for the 49 DOF renormalization.

The procedure for solving the initial-value problem is to accept the results of the renormalization as the starting values of the next phase of the integration process. The results of following this procedure are shown in figure 5. We show separately the time histories of E, E_1 and E_2. The representation was renormalized at time intervals of $0{\cdot}2/(u_0 k_0)$. Also shown in the figure (dashed lines) are the extensions of the curves which would have occurred in the absence of renormalization. The total energy decay, in the absence of renormalization, shows a tendency to level off. With renormalization, on the other hand, the decay rate seems to be sustained at a more even rate. Perhaps this phenomenon indicates that, as the second term grows beyond the minimum required

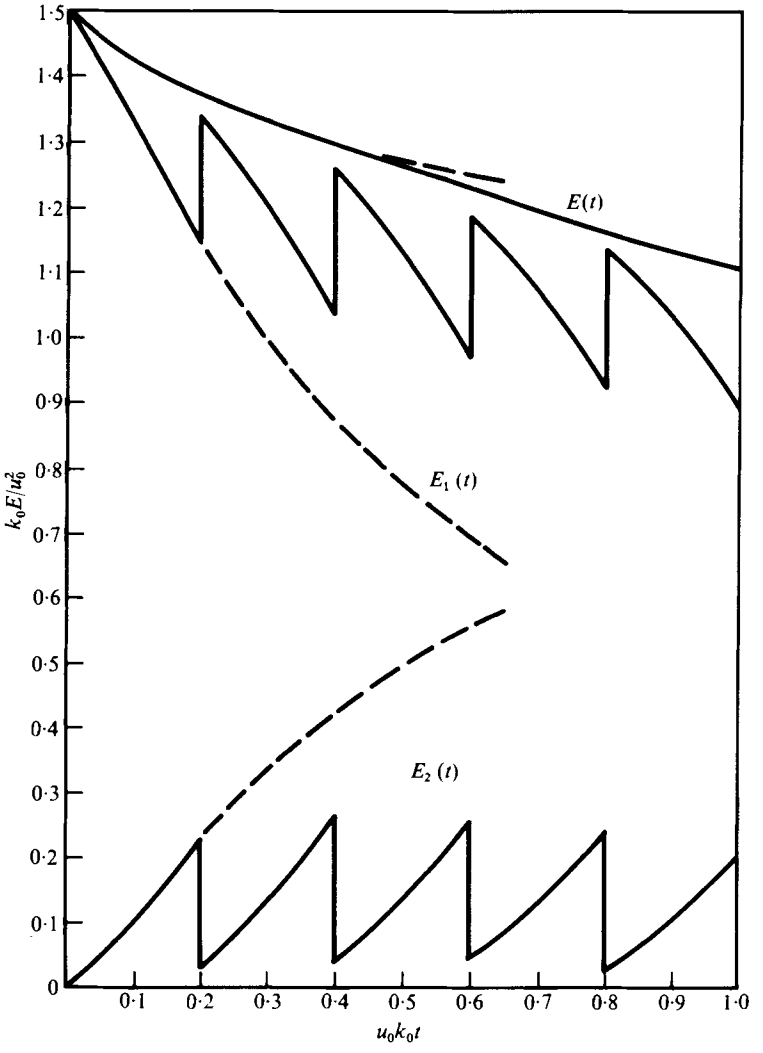

FIGURE 5. Energy time histories for initial Reynolds number of 1000. The solid lines are the results of using renormalization. The dashed lines are the results obtained without renormalization.

to capture the inherent non-Gaussianity, the anomalous second-term contribution detracts from the ability to transfer energy.

Further evidence that the energy decay is nearly correct for this case is given in figure 6. This figure is a plot of $E(0)/E(t)$ *vs.* time. It has been observed in the past (Batchelor 1960, p. 135) that this quantity should grow linearly with time. It seems reasonable to conclude that the computed results presented here are following that same trend, as opposed to the results without renormalization, which again show a levelling-off effect.

Furthermore, consider figure 7. This figure is a plot of the dimensionless dissipation rate, $A = (L_p/u^3)du^2/dt$, found (Batchelor 1960, p. 106) to be of order unity. The result shown in figure 7 justifies the conclusion that the rate of energy dissipation is correctly calculated here. This is a property which was never achieved in the many studies of Burgers model turbulence.

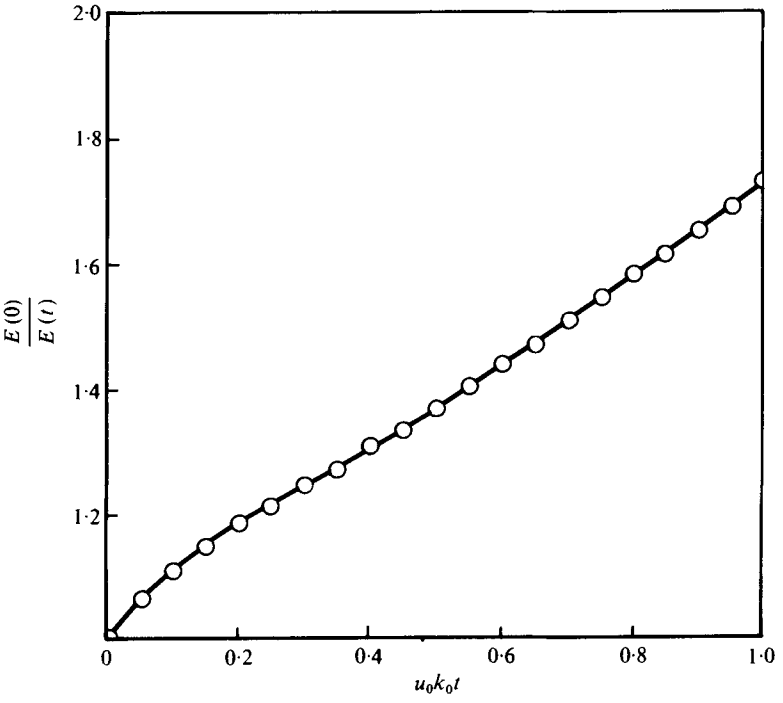

FIGURE 6. Plot of $E(0)/E(t)$ *vs.* time for initial Reynolds number of 1000. Linear growth agrees with experimental observations.

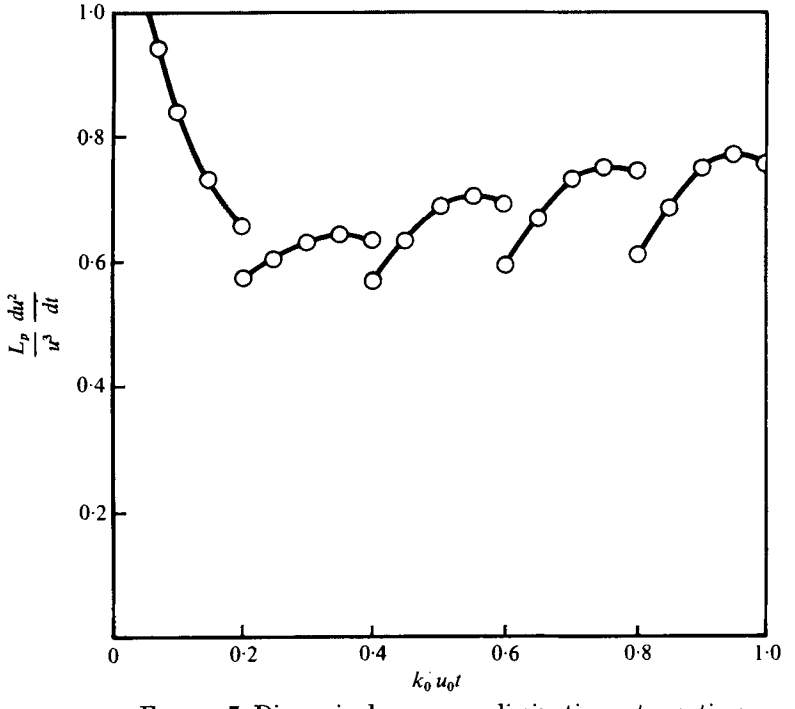

FIGURE 7. Dimensionless energy dissipation rate *vs.* time for initial Reynolds number of 1000.

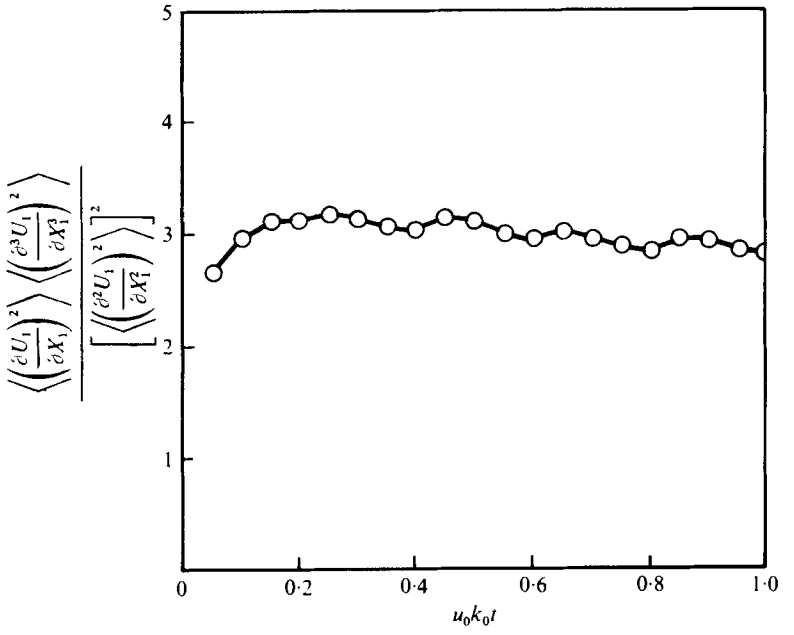

FIGURE 8. Dimensionless combination of second-order movements *vs.* time for initial Reynolds number of 1000.

Two other quantities, which were measured by the early workers in turbulence (Batchelor 1960, p. 118), are shown in figures 8 and 9. First, figure 8 is a plot of the dimensionless ratio

$$\frac{\left\langle \left(\frac{\partial u_1}{\partial x_1}\right)^2 \right\rangle \left\langle \left(\frac{\partial^3 u_1}{\partial x_1^3}\right)^2 \right\rangle}{\left[\left\langle \left(\frac{\partial^2 u_1}{\partial x_1^2}\right)^2 \right\rangle\right]^2} = \frac{35}{27} \frac{\int_0^\infty k^6 E(k)\,dk \int_0^\infty k^2 E(k)\,dk}{\left[\int_0^\infty k^4 E(k)\,dk\right]^2}$$

as a function of time. This quantity is very stable with a value of about 3. Batchelor (1960, p. 118) presents measurements of the same quantity showing it to range from about 3 for low Reynolds number to about 4 for high Reynolds number. Figure 9 is a plot of the dimensionless third-order moment

$$-S_0 = \frac{\left\langle \left(\frac{\partial u_1}{\partial x_1}\right)^3 \right\rangle}{\left[\left\langle \left(\frac{\partial u_1}{\partial x_1}\right)^2 \right\rangle\right]^{\frac{3}{2}}} = -\tfrac{3}{7}(30)^{\frac{1}{2}} \nu \frac{\int_0^\infty k^4 E(k)\,dk}{\left[\int_0^\infty k^2 E(k)\,dk\right]^{\frac{3}{2}}}$$

as a function of time. This quantity is somewhat more erratic but is consistent with the findings of Batchelor (1960, p. 118), who shows a value of 0·3 for high Reynolds number turbulence.

All of the results presented thus far have been derived from initial conditions chosen to be near the expected equilibrium solution. Using the fixed base or the moving base analysis, it was not usually possible to start in a configuration far from equilibrium. The expectation has been that the renormalization, on the other hand, would allow the

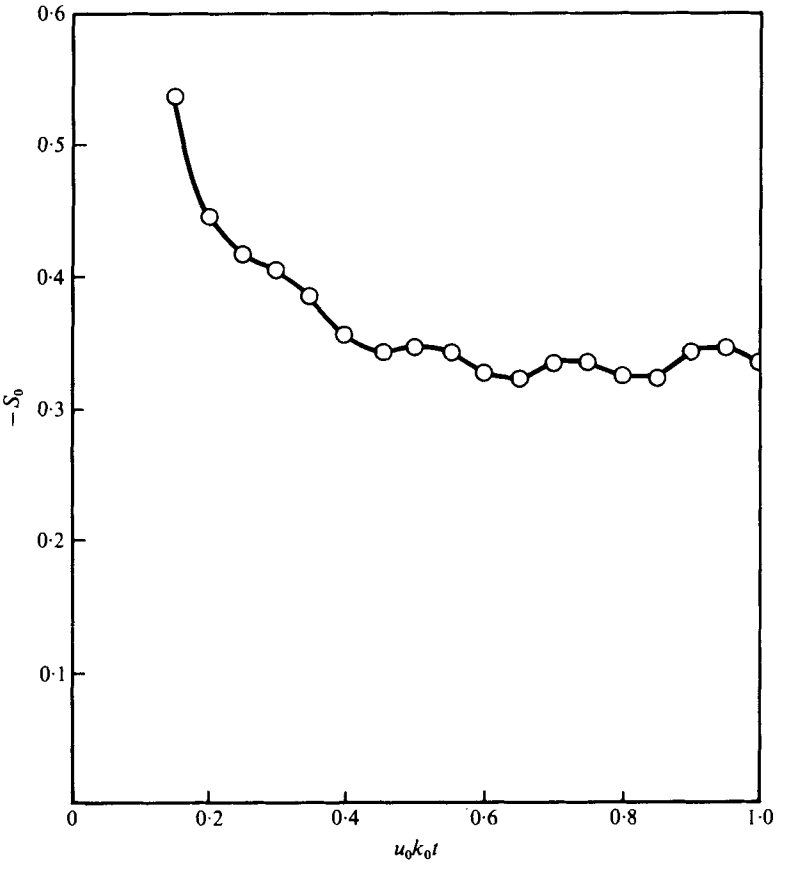

FIGURE 9. Dimensionless third-order moment *vs.* time for initial Reynolds number of 1000.

calculation to proceed even when the initial conditions are highly non-equilibrium. The following two examples have been chosen to demonstrate this capability. In each example, the problem solved is basically the same as the previous case (Reynolds number of 1000) but the initial spectrum is perturbed from the Kolmogorov spectrum in the inertial subrange. In the first case, the initial spectrum has a spike superimposed on the otherwise Kolmogorov inertial subrange. In the second example, a dip is superimposed on the inertial subrange. In each case, it is expected that the evolution of the process will proceed to remove the perturbation.

Figure 10 is a plot of the inertial-subrange portion of the spectrum which initially had a spike. It is clear that the process is trying to remove the spike. The short term effect of the spike is to produce waves in the inertial subrange. Ultimately, however, the waves die out and a nearly Kolmogorov spectrum is recovered. Figure 11 shows essentially the same results for the initial spectrum with a dip in the inertial subrange. For comparison, figure 12 is a plot of the corresponding result for the initial spectrum with no perturbation.

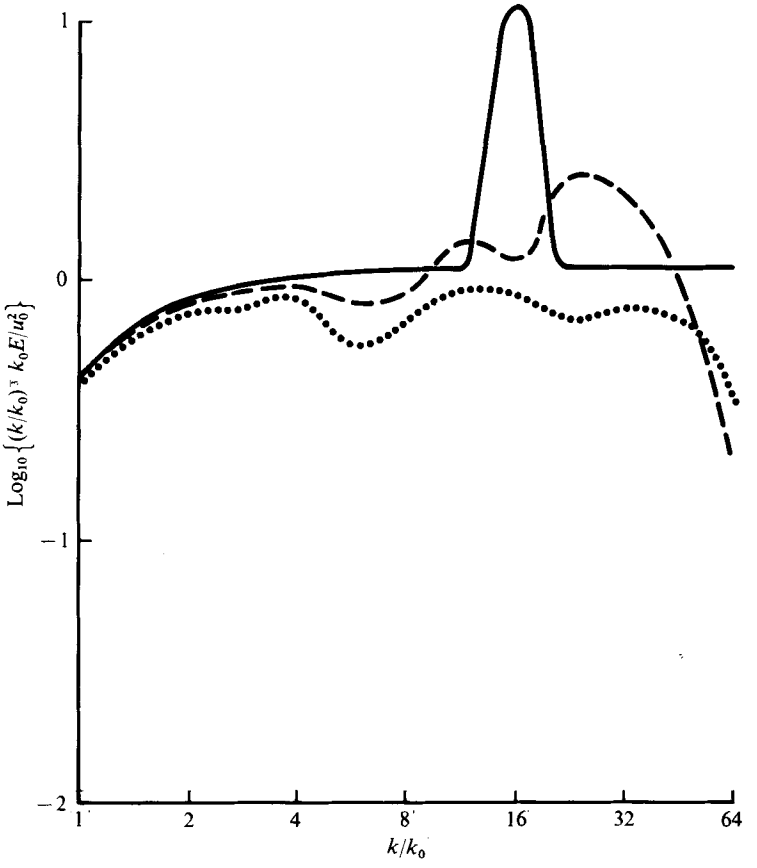

FIGURE 10. Evolution of spectrum that initially had a bump in the inertial subrange. ——, initial spectrum; – – –, spectrum at time $u_0 k_0 t = 0{\cdot}3$; · · · ·, $u_0 k_0 t = 0{\cdot}6$.

9. Calculation of flatness factor

Fundamental to the WH expansion is the assumption that turbulence is nearly Gaussian. It has been shown previously that the third-order moments [e.g. $T(k)$] are small. As a check on the near Gaussianity of the turbulence (and in particular the WH representation) consider the flatness factor of u_1, the first component of the velocity vector:

$$\text{F.F.} = \langle u_1^4 \rangle \langle u_1^2 \rangle^{-2}. \tag{9.1}$$

We expect to find a value near 3, the flatness factor of a Gaussian random variable.

To evaluate the flatness factor in terms of the WH kernels we first note that the second-order moment is simply related to the total energy by

$$\langle u_1^2 \rangle = \tfrac{2}{3}E = \tfrac{2}{3}\int_0^\infty E(k)\,dk. \tag{9.2}$$

The fourth-order moment consists of three types of combinations of first and second kernels as follows:

$$\langle u_1^4 \rangle = \langle u_1^4 \rangle^{(0)} + \langle u_1^4 \rangle^{(2)} + \langle u_1^4 \rangle^{(4)}, \tag{9.3}$$

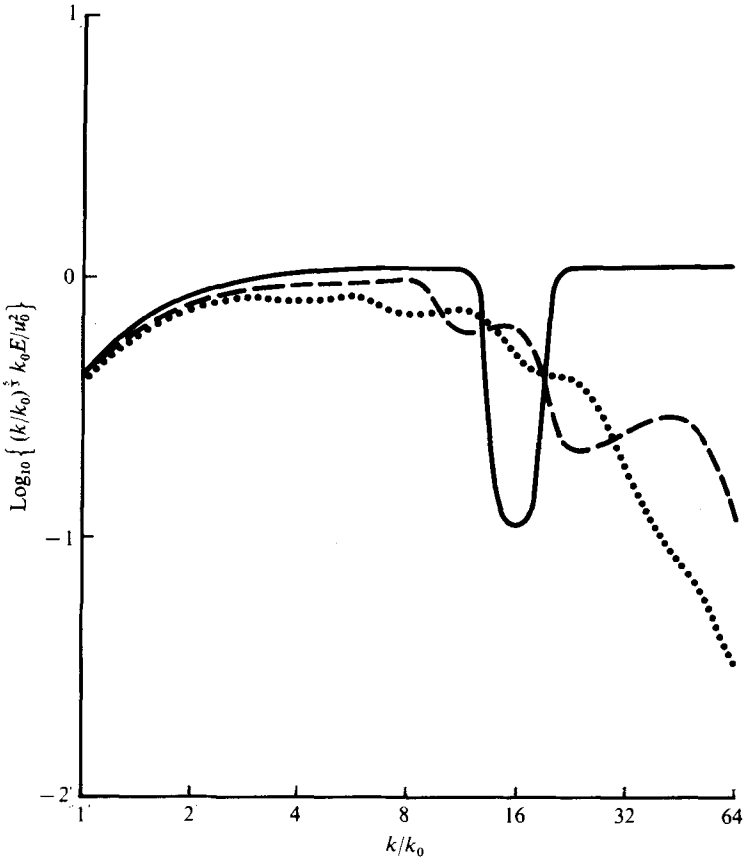

FIGURE 11. Evolution of spectrum that initially has a dip in the inertial subrange. ——, initial spectrum; – – –, spectrum at time $u_0 k_0 t = 0{\cdot}3$; · · · ·, $u_0 k_0 t = 0{\cdot}6$.

where $$\langle u_1^4\rangle^{(n)} = O(\{K^{(1)}\}^{4-n}\{K^{(2)}\}^n).$$

The zeroth-order term is simply related to the first kernel energy as follows:

$$\langle u_1^4\rangle^{(0)} = \tfrac{4}{3}E_1^2. \tag{9.4}$$

The second-order term is found to be

$$\langle u_1^4\rangle^{(2)} = \tfrac{8}{3}E_1 E_2 + \tfrac{48}{15}(I_1 + I_2 + I_3), \tag{9.5}$$

where
$$I_1 = (2\pi)^{-3}\int C_{ijl}(\mathbf{k})\, C_{ijl}(\mathbf{k})\, d\mathbf{k},$$
$$I_2 = (2\pi)^{-3}\int C_{iil}(\mathbf{k})\, C_{jjl}(\mathbf{k})\, d\mathbf{k},$$
$$I_3 = (2\pi)^{-3}\int C_{ijl}(\mathbf{k})\, C_{jil}(\mathbf{k})\, d\mathbf{k},$$

and
$$C_{ijl}(\mathbf{k}) = -i(2\pi)^{-3}\int K_{ia}^{(1)}(\mathbf{k}_1)\, K_{ja}^{(2)}(\mathbf{k}_1, \mathbf{k})\, d\mathbf{k}_1.$$

We shall not attempt to calculate the term which is fourth-order in the second kernel. To do so would be a laborious calculation and should contribute very little to the final answer.

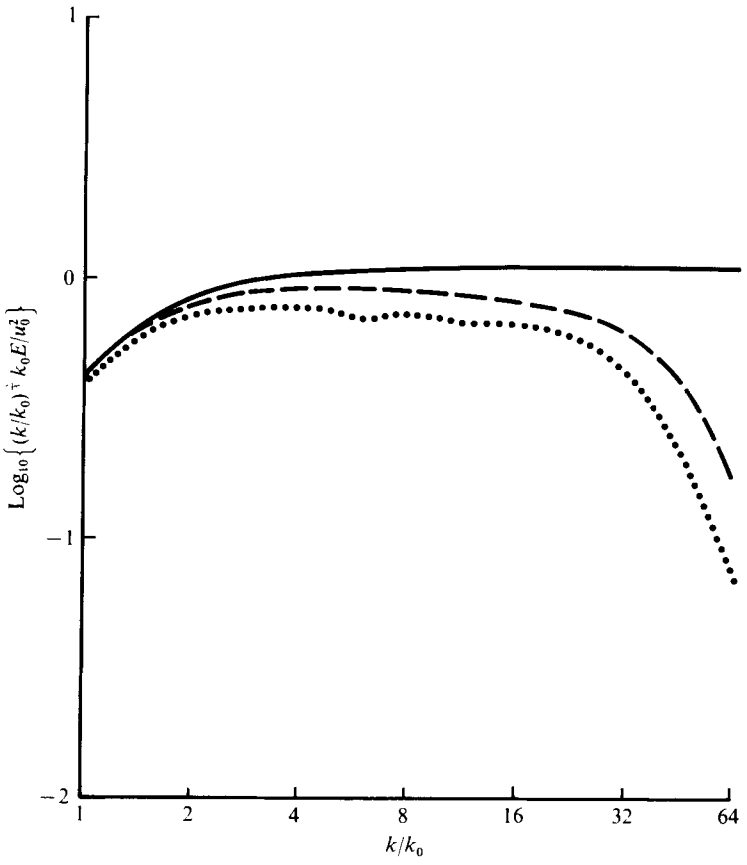

FIGURE 12. Evolution of spectrum that initially has no disturbance in the inertial subrange. ——, initial spectrum; – – –, spectrum at time $u_0 k_0 t = 0{\cdot}3$; · · · ·, $u_0 k_0 t = 0{\cdot}6$.

The flatness factor was calculated for the $Re = 1000$ case presented earlier and the results are given in figure 13. Plotted separately as functions of time are F.F., F.F.$^{(0)}$, and F.F$^{(2)}$, where

$$\left.\begin{aligned} \text{F.F.}^{(0)} &= \langle u_1^4 \rangle^{(0)} \langle u_1^2 \rangle^{-2}, \\ \text{F.F.}^{(2)} &= \langle u_1^4 \rangle^{(2)} \langle u_1^2 \rangle^{-2}, \end{aligned}\right\} \tag{9.6}$$

and

$$\text{F.F.} = \text{F.F.}^{(0)} + \text{F.F.}^{(2)}.$$

The dashed lines indicate the breaks at which the calculation was renormalized. Notice that the total flatness factor remains near the Gaussian value of 3 for all time. The contributions to the total, on the other hand, are not at all constant. The zeroth-order contribution starts out large but rapidly decreases while the second-order contribution starts out small and increases. This behaviour indicates the rapid shift in the content of the WH expansion from the first term to the second term even though the random process remains nearly Gaussian. The effect of renormalization is to put as much as possible of the total energy back into the first term. The fact that the total flatness factor changes when the process is renormalized probably indicates the extent to which fourth-order moments are changed by renormalization. Recall that the

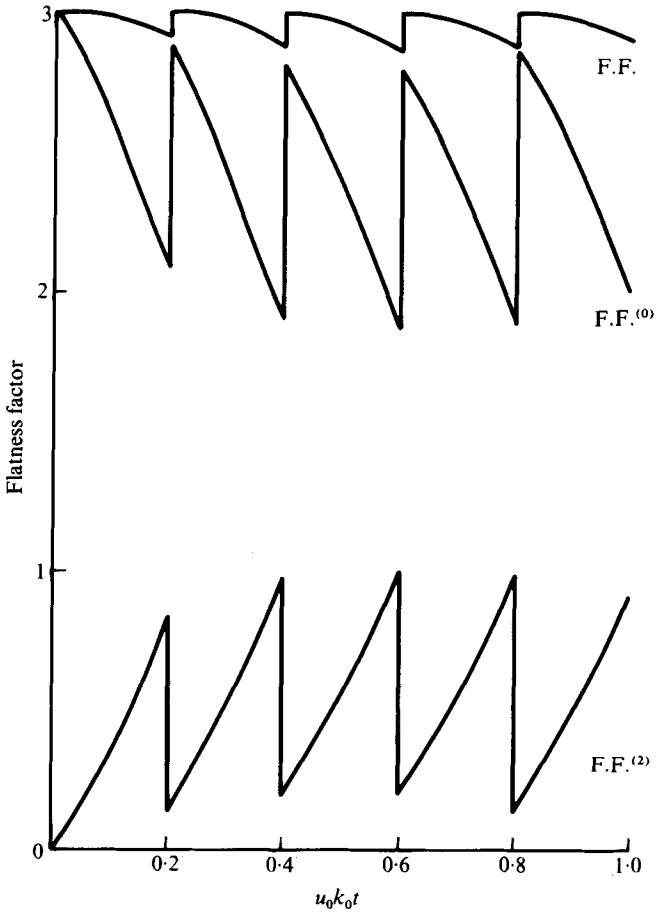

FIGURE 13. Flatness factor *vs.* time for initial Reynolds number of 1000. Also shown are zeroth-order and second-order contributions.

process was designed to be measure-preserving only up to third order. The error introduced in the fourth-order moment by renormalizing appears to be about 5 %. It is also possible that the neglected fourth-order term ($F.F.^{(4)}$) could be contributing somewhat to a change in flatness factor due to renormalization.

10. Concluding remarks

It has been shown that significant results can be obtained from the moving base WH expansion for limited decay times. For fluctuation Reynolds numbers up to 10000 (mean flow Reynolds numbers of a half million) it is possible to calculate (to within experimental error) the Kolmogorov constant and the viscous-range spectral behaviour. It is necessary to begin the calculation with the five-thirds spectrum but the equilibrium form is preserved. The calculation is completely deductive, of course, and hence requires no adjustable parameters. Furthermore, by using the renormalization scheme, the calculation can be extended to decay times larger than those possible with the moving base expansion alone and can be started from initial spectra other

than the Kolmogorov form. The resulting calculation procedure is thus a solution to the problem of decaying isotropic turbulence (assuming it is possible to continue renormalizing as long as necessary). Further work is required to define the limitations of this procedure. In addition, the flatness factor of the turbulence was calculated. It should be noted that production runs on the UCLA IBM 360/91 digital computer cost typically but \$20–30.

It is a pleasure to acknowledge partial support from the NASA Ames Research Center. Portions of this research were presented at the 14th International Congress of Theoretical and Applied Mechanics, Delft, Netherlands, 30 August to 4 September 1976. Many of the discussions presented here can be found in greater detail in Hogge (1977).

REFERENCES

BATCHELOR, G. K. 1960 *The Theory of Homogeneous Turbulence.* Cambridge University Press.

BODNER, S. E. 1969 Turbulence theory with a time-varying Wiener–Hermite basis. *Phys. Fluids* **12**, 33.

CANAVAN, G. H. 1970 Some properties of a Lagrangian Wiener–Hermite expansion. *J. Fluid Mech.* **41**, 405.

CAMERON, R. H. & MARTIN, W. T. 1947 The orthogonal development of non-linear functionals in series of Fourier–Hermite functions. *Ann. Math.* **48**, 385.

CLEVER, W. C. & MEECHAM, W. C. 1972 Time-dependent Wiener–Hermite base for turbulence. *Phys. Fluids* **15**, 244.

CROW, S. C. & CANAVAN, G. H. 1970 Relationship between a Wiener–Hermite expansion and an energy cascade. *J. Fluid Mech.* **41**, 387.

DOI, M. & IMAMURA, T. 1969 The Wiener–Hermite expansion with time-dependent ideal random functions. *Prog. Theor. Physics (Kyoto)* **41**, 348.

GRANT, H. L., STEWART, R. W. & MOILLIET, A. 1961 Turbulence spectra from a tidal channel. *J. Fluid Mech.* **12**, 241.

HOGGE, H. D. 1977 The Wiener–Hermite expansion applied to decaying isotropic turbulence using a renormalized, time dependent base. Ph.D. thesis, University of California, Los Angeles.

IMAMURA, T., MEECHAM, W. C. & SIEGEL, A. 1965 Symbolic calculus of the Wiener process and Wiener–Hermite functionals. *J. Math. Phys.* **6**, 695.

JENG, D.-t., FOERSTER, R., HAALAND, S. & MEECHAM, W. C. 1966 Statistical initial-value problem for Burgers' model equation of turbulence. *Phys. Fluids* **9**, 2114.

KISTLER, A. L. & VREBALOVICH, T. 1966 Grid turbulence at large Reynolds number. *J. Fluid Mech.* **26**, 37.

MEECHAM, W. C. 1972 Renormalization for the Wiener–Hermite representation of statistical turbulence. *Prog. Geophys.* **18**, 445.

MEECHAM, W. C. & CLEVER, W. C. 1971 Use of the C–M–W representation for nonlinear random process applications. *Lecture Notes in Physics: Statistical Models and Turbulence*, p. 205. Springer.

MEECHAM, W. C., IYER, P. & CLEVER, W. C. 1975 Burgers' model with a renormalized Wiener–Hermite representation. *Phys. Fluids* **18**, 1610.

MEECHAM, W. C. & JENG, D.-t. 1968 Use of the Wiener–Hermite expansion for nearly normal turbulence. *J. Fluid Mech.* **32**, 225.

ORSZAG, S. A. & BISSONNETTE, K. R. 1967 Dynamical properties of truncated Wiener–Hermite expansions. *Phys. Fluids* **10**, 2603.

WIENER, N. 1939 The use of statistical theory in the study of turbulence. *Proc. 5th Int. Cong. Appl. Mech.* p. 356. Wiley.

WIENER, N. 1958 *Nonlinear Problems in Random Theory.* M.I.T. Press.